Journal of Materials Chemistry A

Accepted Manuscript

ROYAL SOCIETY OF CHEMISTRY

www.rsc.org/materialsA

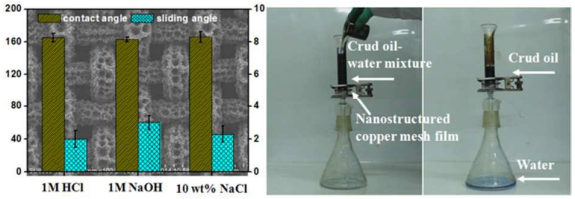

A novel oil/water separation copper mesh film with special anti-corrosive ability was prepared by a simple electrodeposition process.

Cite this: DOI: 10.1039/c0xx00000x

www.rsc.org/xxxxxx

ARTICLE TYPE

Anti-corrosive hierarchical structured copper mesh film with superhydrophilicity and underwater low adhesive superoleophobicity for highly efficient oil/water separation

Enshuang Zhang,[a, ‡] Zhongjun Cheng,*[b, ‡] Tong Lv,[a] Yihao Qian[a] and Yuyan Liu*[a]

Received (in XXX, XXX) Xth XXXXXXXXX 20XX, Accepted Xth XXXXXXXXX 20XX
DOI: 10.1039/b000000x

Recently, oil/water separation is becoming a feverish subject due to the increasing oil spill accidents. Separating films with underwater superoleophobicity have aroused much interest due to its special oil-repellent and anti-fouling property. Good environmental stability such as anti-corrosive ability is very important for these films in practical application because water contacts these films intimately during the separating process. Until now, almost all reported separating films with anti-corrosive ability are made of polymer, and related inorganic separating materials are still rare. In this work, through a simple electrodeposition process, a novel porous structured copper mesh film was prepared. The film shows superhydrophilicity in air and low-adhesive superoleophobicity in water. Using the film for oil/water separation, the separation efficiency is higher than 99% for various oil/water mixtures. Importantly, after immersion into corrosive solutions such as acid and basic solutions, the wetting properties and the separating performances of the film have no apparent variation, indicating that the as-prepared film has a good environmental stability. This paper report a new separating film for oil/water mixture, the special anti-corrosive property allows it to be used in many other practical applications, such as anti-fouling, filtration and sewage treatment.

Introduction

In the past decades, lots of oil spill accidents have aroused people's attention on the marine environment and aquatic ecosystem. Separation of oil/water mixture becomes a global challenge.[1,2] Traditional separating methods including gravitational separation, coagulation, flocculation, and air flotation are limited by energy-cost, low separation efficiency, and complex separation process, and new functional materials that can achieve efficient oil/water separation are highly desired.[3] Because of different interfacial effect of water and oil, design and fabrication of novel interfacial materials with special wetting behaviors would be promising to solve the problem.[4, 5]

Recently, materials with both superhydrophobicity and superoleophilicity have aroused much interest because they can realize filtration or absorb of oil from water.[6-39] Some examples include polytetrafluoroethylene coated stainless steel mesh film,[10] carbon nanotubes film,[11] multifunctional foam,[12, 22] and polydimethysiloxane (PDMS) coated nanowire membrane.[21] Noticeably, all these "oil-removal" type materials are easily fouled or even blocked by oils, which would affect the separation capacity and reusing of these films. In order to overcome these disadvantages, Jiang et al. advanced a new hydrogel coated film, which shows superhydrophilicity and underwater superoleophobicity.[40] Using such film to separate oil/water mixture, water can pass through the film while oil would be retained. Such "water-removal" type design gives us a new avenue to prepare oil/water separating film.[41-49] For example, Gao et al. reported a dual-scaled porous nitrocellulose membrane with high efficient oil/water separating ability;[41] Feng et al. prepared a thermo and pH dual-responsive hydrogel membrane, on which, the separating process can be controlled under external stimulus;[47] Liu et al. realized the oil/water separation on the poly(sulfobetaine methacrylate) grafted glass fiber filter;[48] Jin et al. fabricated $Cu(OH)_2$ coated copper mesh film, which also shows high efficient oil/water separating property.[44] It is worthy of noting that for these "water-removal" separating films, the stability of the film in water with complex conditions such as strong acid and strong alkaline are very important for the practical applications, because water contacts these films intimately during the separating process. However, such anti-corrosive films only were reported on the polymers or polymer coated materials with limited selectable options.[39, 41, 45] In addition, polymeric materials have certain weakness on consideration of practical application, such as high cost and tedious preparation process.

In this paper, through a simple electrodeposition process, we prepared a new inorganic hierarchical structured copper mesh oil/water separation film, which shows superhydrophilicity and underwater low-adhesive superoleophobicity. Using the as-obtained film for oil/water separation, the mixture can be separated with high efficiency. It should be mentioned that oil/water separation on inorganic $Cu(OH)_2$ coated copper mesh

film have be realized,[44] however, the $Cu(OH)_2$ nanostructures would be destroyed in strong acid water solution, and the separation ability would be lost. Herein, on our film, the wetting properties and separation effect have no apparent variation after immersion in corrosive water (including strong acid water, strong basic solution, and salty solution), indicating that the film has a special environmental stability, which promises the film be used in more complex applications.

Experimental section

Fabrication of hierarchical structures on the copper mesh substrate

The hierarchical structures on the copper mesh film were fabricated through a simple electrodeposition process, which is similar as previous reports. [50] Briefly, the pre-cleaned copper meshes substrates with different pore sizes were cut into small pieces and used as the cathodes. Pt plate ($\approx 2 \times 2$ cm^2) was used as the anode. The electrolyte was the water solution containing 0.1 M $CuSO_4$ and 1 M H_2SO_4. The electrodeposition process was conducted on a device (dc power KXN - 6020 - D, shenzhen zhaoxin electronic instrument equipment factory). The current density is constant at 6 A cm^{-2} and the electrodeposition time is varied between 5 to 15 s. Finally, the substrates were washed with deionized water and dried under nitrogen blow.

Oil/water separation experiment

The hierarchical structured copper mesh film was fixed between two glass tubes. Before the separation, the film was firstly wetted by water and then the oil/water mixture (V_{water}/V_{oil} = 3 : 1) was poured into the upper tube. At last, the separation process was achieved by the weights of the liquids.

Instruments and characterization

The contact angles and sliding angles were investigated on a contact angle meter (JC 2000D5, Shanghai Zhongchen Digital Technology Apparatus Co., Ltd.). For water and oil contact angle measurement in air, liquid droplets were directed put on the film. For underwater oil wetting performance measurement, the substrates were firstly fixed in a quartzose container that is transparent and full of water. For 1, 2-dichloroethane with higher density than water, the oil droplet was directly put on the film. For oils with lower density than water, such as petroleum ether, the oil droplet was released under the film through an inverted needle (more details see supporting information Scheme 1). The average values were achieved by examining five points on the identical film. The rolling angles were investigaed by tilting the film with a dropler (4 μL) that contact with the film until the droplet started to slide. The oil-adhesive forces were measured on a high-sensitivity microelectromechanical balance system (Dataphysics DCAT 11, Germany). An oil droplet (5 μ L) was suspended with a metal cap and controlled to contact with the film which were placed underwater at a constant speed of 0.01 mm s^{-1} and then to leave. The forces were recorded during the entire time. The morphology on the substrates was obtained on a scanning electron microscope (HITACHI, SU8000). Corrosive liquids were water solution containing HCl, NaOH and NaCl, respectively. The water pH was measured on a pH meter (PB-10, sartorius). Photographs in Figure 4 were obtained on a camera (Canon HF M41). The oil concentration was analyzed using an Infrared Spectrometer Oil Content Analyzer (CY2000, China). X-ray diffraction spectroscopy data were carried out by using an X-ray diffractometer model D8 advance (Bruker) with Cu Kα radiation (λ = 1.5418 Å).

Results and discussion

In this work, copper mesh was used as the separating substrate for its widely application in our daily life. Figure 1a shows the typical scanning electron microscopy (SEM) image of original copper mesh substrate. One can observe that smooth copper wires weave together and form the reticulated structure. The average diameter of the copper wires is about 78 μm (Figure 1b). After electrodeposition (Figure S1 in supporting information), the diameter of the copper wires is increased to about 138 μm (Figure 1c), and porous structures with an average pore size of about 23 μm can be seen on the copper wires (Figure 1d). Amplified image shows that these pores are composed of dendritical aggregates (Figure 1e), and these aggregates are made up of nanoparticles with average diameter of about 485 nm (inset in Figure 1e). Figure 1f displays the XRD pattern of the obtained film, from which, one can find that only peaks ascribed to Cu can be observed, indicating that the as-prepared nanostructures are elementary Cu, which is consistent with the energy dispersive spectroscopy (EDS) results (Figure S2 in supporting information). From the above, it can be concluded that through a simple electrodeposition process, hierarchical structured elementary Cu can be produced on the copper mesh substrates. As reported, such hierarchical structures can amplify the surface wetting performance,[51-55] and it is expected that particular wetting performances can be observed on the as-prepared film.

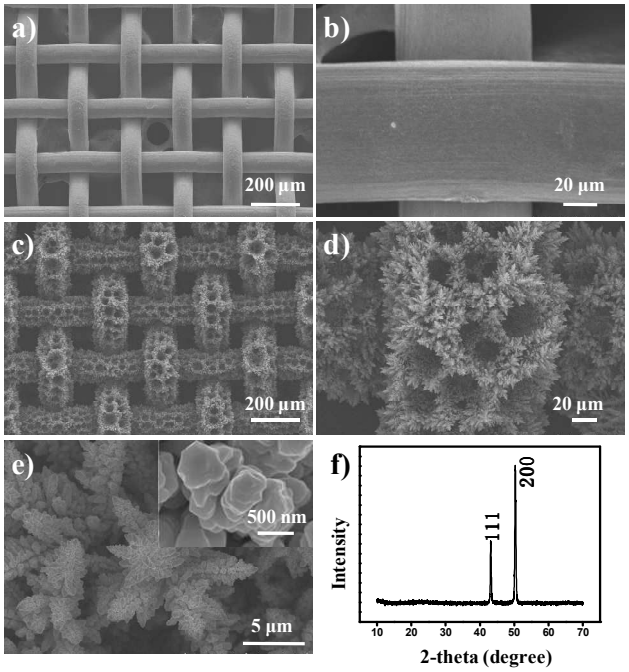

Figure 1. (a, b) SEM images of the copper mesh substrate with low and high magnification, respectively. (c-e) SEM images of nanostructured copper mesh film with different magnifications. (f) XRD patterns of the substrate after electrodeposition, indicating that only elementary copper nanostructures were produced.

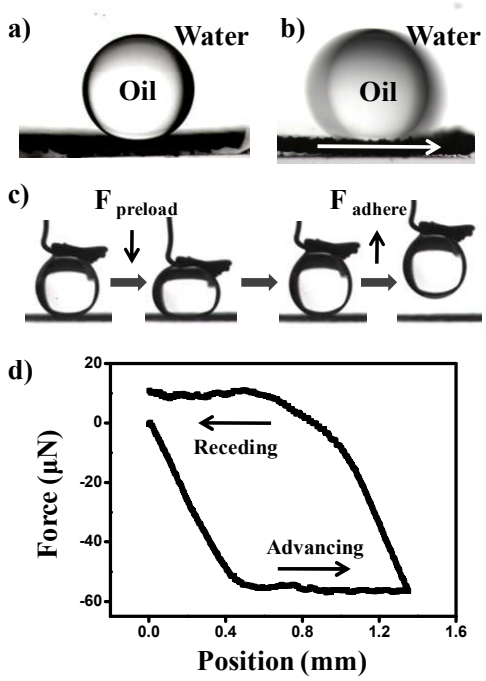

Figure 2. (a) Shape of an oil droplet (4 μL, 1, 2-dichloroethane) on the nanostructured copper mesh film in water with a contact angle of about 162°. (b) An oil droplet rolling away the film with a low sliding angle less than 2°. (c) Photographs of the dynamic underwater oil-adhesion measurement on the nanostructured film. An oil droplet was used as the detecting probe to contact the film and then leave, it can be seen that the film exhibit ultralow affinity to the oil droplet. (d) Force-distance curves recorded before and after the oil droplet contact the film in water.

Using a contact angle measure meter, the wetting properties of the obtained film were investigated comprehensively. In air, the as-prepared film shows superhydrophilicity and superoleophilicity (Figure S3 in supporting information). After immersion into water, the phenomenon would be different, and the film displays superoleophobicity. As shown in Figure 2a, an oil droplet (4 μL, 1, 2-dichloroethane) can stand on the film with a contact angle of about 162°, indicating that the film is underwater superoleophobic. Meanwhile, the film shows low adhesion to the oil, and the oil droplet can roll away the film with an extremely low sliding angle (less than 2°, Figure 2b). In order to further examine the oil-repellent ability of the film, an oil droplet was used to contact the film and then allowed to leave. As shown in Figure 2c, even at a certain pressure, the oil droplet can still leave the film easily without any residual, indicating that the film has an ultralow adhesion. Through a high sensitivity microelectromechanical balance system, the oil adhesion force of the obtained film was further measured, and the adhesive force is too low to be detected (less than 1 μN, Figure 2d). In addition to 1, 2-dichloroethane, some other oils such as diesel, gasoline, and hexadecane were also used to test the oleophobicity of the film. As shown in Figure 3, all the oil contact angles are larger than 150° and all the sliding angles are lower than 2°, means that the film shows good underwater superoleophobicity and low adhesion regardless of oil types. The wetting performances of the films were also related to the pore size on the substrates. The hierarchical structured Cu coated substrates with pore size between 48 μm and 420 μm were tested (Figure S4 in supporting information). One can find that films obtained on substrates with pore sizes below 200 μm are ideal, and underwater superoleophobicity can be realized on these films.

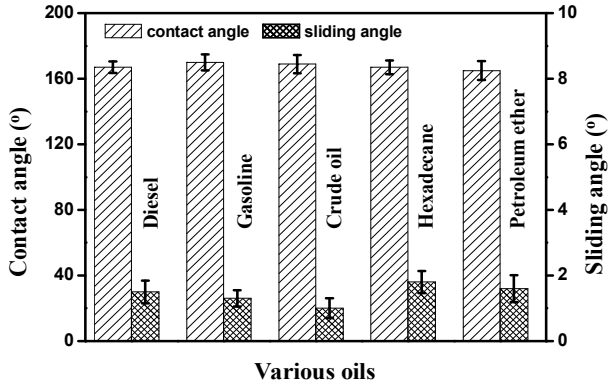

Figure 3. Statistic of contact angles and sliding angles for various oils on the nanostructured film in water.

As previously reported, films with superhydrophilicity and underwater superoleophobicity can be used in the oil/water separation. To test the separating ability of our film, a series proof-of-concept studies were carried out. The separating process is displayed in Figure 4. The separating film was firstly fixed between two glass tubes (Figure 4a), mixture of water and crude oil was poured into the upper tube (before adding the mixture, the separating film was first wetted by pure water). It can be seen that without external force, water can permeate the film due to the superhydrophilicity of the film (the colour of water for the presence of methylene blue). Noticeably, since the underwater superoleophobicity, oil cannot pass through the film and be kept above the film (more details see Figure S5, movie 1, movie 2, and movie 3 in supporting information). These results indicate that using the as-prepared film, oil/water mixture can be separated easily. Some other mixtures of water and oils including diesel, gasoline, hexadecane, and petroleum ether were also used to investigate the separating ability of the film, and all these mixtures can be separated successfully, indicating that the as-prepared film has a wide range of applications. Furthermore, after

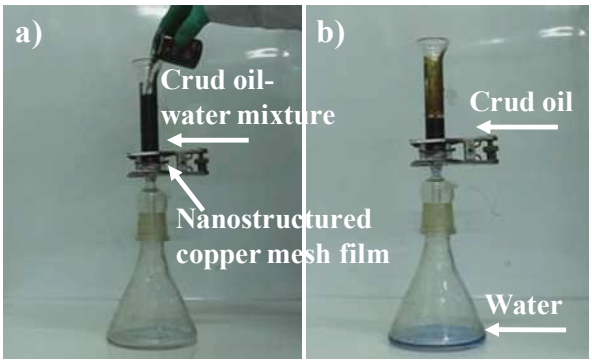

Figure 4. Oil/water separation on the hierarchical structured film: (a) the film was clamped between two glass tubes, the mixture of water and crude oil was poured into the upper tube (before adding the mixture, the film was firsted wetted by water), (b) water permeated through the film and the oil was retained in the upper tube (the colour of water for the presence of methylene blue), demonstrating the oil/water mixture can be separated using the as-prepared film.

separation, the film can be cleaned easily for reuse, and the film can remain underwater superoleophobicity and low adhesions even after 30 times use, showing a good stability.

The separation efficiency was also examined. By using the infrared spectrometer oil content analyzer, the oil contents before and after separation were measured, and the separation efficiency can be obtained according to the following equation;[40]

$$R\% = (1 - \frac{C_p}{C_o}) \times 100\% \qquad (1)$$

Here C_o and C_p are the oil concentration of original oil/water mixture and collected water after separation, respectively. As shown in Figure 5, the separation efficiency is higher than 99% for all used oil/water mixture.

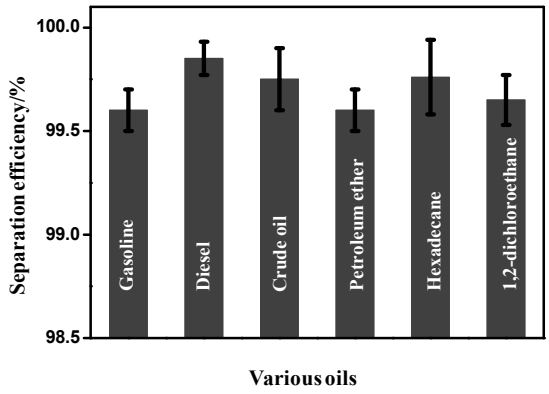

Figure 5. The separation efficiency of the nanostructured film for various oils in terms of their oil rejection coefficient.

In addition to the separation efficiency, the intrusion pressure, in other words, the maximum pressure that the film can support was also investigated. The intrusion pressure is provided by the weight of oil, thus, the experimental value can be obtained according to the equation:

$$P_{\exp} = \rho g h_{\max} \qquad (2)$$

Where P_{exp} is the experimental intrusion pressure, ρ is the density of the oil, g is the acceleration of the gravity, and $h_{\max}$ is the maximum height of the oil that the film can support. Figure 6 shows the statistic of the intrusion pressure for various oils, it can be seen that the average intrusion pressure for all these oils are above 1.0 kPa, demonstrating that our separating device has a good stability.

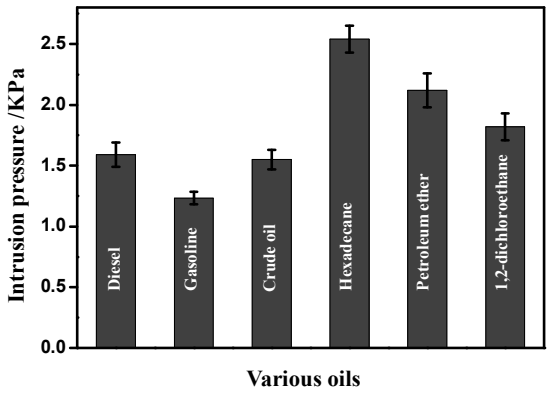

Figure 6. Experimental values of intrusion pressures for different oils.

In practical applications, the environmental stability of the separating film is vital important. As for these "water-removal" type materials, because water will contact with these films intimately during the separating process, the stability of the film to corrosive liquid such as strong acid and strong basic water solution would be more important. Noticeably, the as-prepared film in this work has such a particular anti-corrosive ability. To evaluate the anti-corrosive ability of the film, the film was firstly immersed into aqueous solution with certain conditions (acid, basic or salt solutions) for about 24 h, and then the oil wetting performances and separation efficiency on the film were examined. It can be seen that for all these water solutions, the underwater superhydrophobicity and low oil adhesions can still be present (Figure 7a), and corresponding separating efficiency retains higher than 99% (Figure 7b, more details see Figure S6-S10, the discussion about oil contact angles in these solutions and the separation efficiency after immersion in corrosive solutions in supporting information), indicating that the obtained film has a good anti-corrosive property.

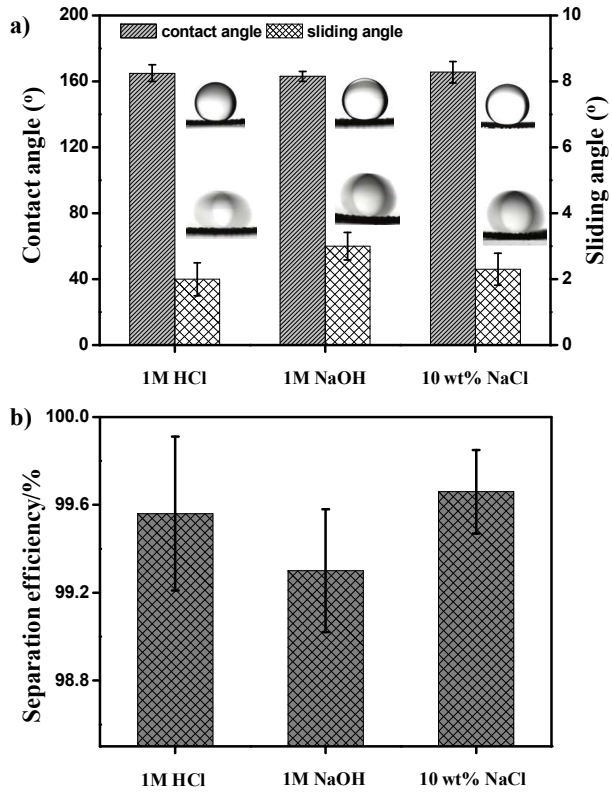

Figure 7. (a) Oil contact angles and sliding angles on the nanostructured film after immersion in HCl, NaOH, and NaCl solutions, respectively. Insets are the photographs on an oil droplet (4 μL, 1, 2-dichloroethane) on the film in corresponding solutions. (b) The separation efficiency of the nanostructured film for gasoline in different corrosive solution in terms of their oil rejection coefficient.

From the above, it can be found that the film's superhydrophilicity and underwater superoleophobicity are the two critical factors for the special separating ability. Because the copper substrate shows hydrophilicity in air (the contact angle on the flat copper surface is about 53°, Figure S11a in supporting information), after introduction of hierarchical structures, the surface hydrophilicity can be intensified according to the Wenzel

equation.[56] As shown in Figure 1, the presence of hierarchical structures can effectively increase the surface roughness. Therefore, water can enter into the hierarchical structures due to the three-dimensional capillary effect and the film would display superhydrophilicity with a contact angle of about 0° (Figure S3a in supporting information). The underwater superoleophobicity can be ascribed to the combined effect of the surface hydrophilicity and the hierarchical structures. When the film was immersed into water, water would enter into the hierarchical structures due to the film's superhydrophilicity (Figure S3a in supporting information). When the oil droplet was placed onto the film, a composite solid/water/oil interface would be formed, and the high oil contact angle can be explained by the following modified equation:[57]

$$\cos\theta_{ow}' = f\cos\theta_{ow} + f - 1 \qquad (3)$$

Here, θ'_{ow} and θ_{ow} are the oil contact angles of an oil droplet contacts with the hierarchical structured copper mesh and flat copper substrates, respectively. f represents the area fraction of copper mesh substrate contacts with oil. In this work, take the 1, 2-dichloroethane as an example, θ'_{ow} = 162° (Figure 2a), θ_{ow} = 120° (Figure S11b in supporting information), and f = 0.098, means that more than 90% contact area is the oil/water contact interface. Therefore, the superoleophobic and easily rolling performances can be observed.

To make the oil/water separation process more clear, we modeled the water and oil wetting processes in Figure 8. In theory, an intrusion pressure ΔP has to be conquered before the liquid can wet the pore bottom since the advancing contact angle θ_A has to be exceeded, which can be described as:[58]

$$\Delta P = \frac{2\gamma}{R} = -l\gamma(\cos\theta_A)/A \qquad (4)$$

Where γ is the surface tension; l is the pore's perimeter; R is the meniscus's radius; A is the pore's area; θ_A is the advancing contact angle on the film. From equation (4), it can be seen that when $\theta_A > 90°$, the film can support certain pressure since the $\Delta P > 0$. In contrast, as the $\theta_A < 90°$, the liquid would get through the film spontaneously as the $\Delta P < 0$. Figure 8a displays a schematic illustration of an intermediate wetting state of water on the film. Because the film is superhydrophilic, θ_A is nearly 0°, the $\Delta P < 0$ and the film cannot support any pressure. When the water contact with the film, it would permeate the film spontaneously as a function of its gravity. When oil contact with the film, as mentioned above, before oil/water separation, the film was firstly wetted by water, and the hierarchical structures would be occupied by water, which can enchance the oil-repellent force. The oil would reside in the composite superoleophobic state, the θ_A is obviously larger than 90°, and $\Delta P > 0$, means that the film can sustain pressure to some extent (Figure 8b). Thus, as shown in Figure 4, oil cannot pass through the film and be retained on the film. According to the above equation, the theoretical maximum pressure that the film can support was also calculated (Figure S12 in supporting information), and it can be seen that the theoretical intrusion pressures are obviously lower than the experimental values. The theoretical intrusion pressure is calculated based on the hypothesis that the only micrometer scale

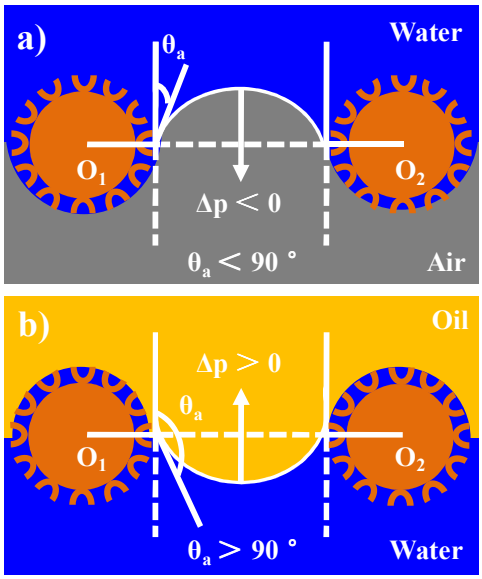

Figure 8. Schematic illustration of liquid-wetting modes: (a) for water, the film shows superhydrophilicity and cannot sustain any pressure because $\Delta p < 0$, thus water can permeate the film spontaneously; (b) for oil, the nanostructures have been occupied by water, the film shows ophobicity, the oil can be supported on the film since the $\Delta p > 0$.

pores poessing the same size with our separating film are present on the substrate.[58] On our separating film, there are lots of hierarchical structures (Figure 1c, 1d), which can capture a lot of water among these structures and help to increase the bearing force (more discussion see supporting information Figure S13 and movie 4). As a result, the obtained experimental intrusion pressures are larger than theoretical values. From the above, it is clear that the superhydrophilicity allows the water permeate the film while underwater superoleophobicity retaines the oil on the film, therefore, oil/water mixture can be separated successfully on such superhydrophilic and underwater superoleophobic film.

Conclusions

In conclusion, a novel hierarchical structured copper mesh film was prepared through a simple electrodeposition process. The film shows both superhydrophilicity and underwater superoleophobicity. Several oil/water mixtures can be separated on the as-prepared film with high efficiency. Importantly, the film has a special anti-corrosive ability, even after immersion into strong acid, strong basic and seawater-like salt solutions, the wetting properties and separating ability of the film have no apparent variation. This paper reports a new functional material to realize the oil/water separation. Since the obtained film has so many virtues including high efficient separating and anti-corrosive abilities, we believe that the film can potentially be used in many other applying fields, such as sewage treatment, microfludic device, and controlled filtration.

Acknowledgements

This work is supported by the National Natural Science Foundation of China (NSFC Grant NO. 21304025); The Fundamental Research Funds for the Central Universities(Grant No.HIT.KISTP.201408); The Research Fund for the Doctoral Program of Higher Education of china (20112302120062). The

assisted project by Heilong Jiang Postdoctoral Funds for scientific research initiation (LBH-Q13063).

Notes and references

[a] *School of Chemical Engineering and Technology, Harbin Institute of Technology, Harbin, Heilongjiang 150001, P.R. China. Fax:(+86)045186402368; Tel: (+86)045186413711; E-mail:liuyy@hit.edu.cn*

[b] *Natural Science Research Center, Academy of Fundamental and Interdisciplinary Sciences, Harbin Institute of Technology, Harbin, Heilongjiang 150090, P.R. China. Fax:(+86)045186412153; Tel: (+86)045186412153;E-mail:chengzhongjun@iccas.ac.cn*

† Electronic Supplementary Information (ESI) available: [SEM images of substrates after electrodeposition for different time; Surface tension of HCl, NaOH, and NaCl solutions; EDs results of the film; water and oil contact angle on the film in air; Dependence of underwater oil contact angle on the pore size of the copper mesh substrates; Oil contact angles and sliding angles on the nanostructured film after immersion in water solutions with pH from 1 to 14; SEM images of nanostructured copper mesh substrates after immersion into corrosive liquid; Photograph of a water droplet and oil droplet on the flat copper film; Theoretical intrusion pressure of different oils on the film; oil/water separation on the copper mesh substrate without nanostructures; movie for the oil/water separation process]. See DOI: 10.1039/b000000x/

‡ These authors contributed equally.

1 M. A. Shannon, P. W. Bohn, M. Elimelech, J. G. Georgiadis, B. J. Mariñas, A. M. Mayes, *Nature*, 2008, **452**, 301.

2 A. K. Kota, G. Kwon, W. Choi, J. M. Mabry, A. Tuteja, *Nat. Commun*, 2012, **3**, 1025.

3 W. Zhang, Z. Shi, F. Zhang, X. Liu, J. Jin, L. Jiang, *Adv. Mater*, 2013, **25**, 2071.

4 4 J. Lahann, *Nat. Nanotechno*, 2008, **3**, 320.

5 5 X. Yao, Y. Song, L. Jiang, *Adv. Mater*, 2011, **23**, 719.

6 6 G. Hayase, K. Kanamori, M. Fukuchi, H. Kaji, K. Nakanishi, *Angew. Chem. Int. Ed*, 2013, **52**, 1986.

7 H. Zhu, D. Chen, N. Li, Q. Xu, H. Li, J. He, J. Lu, *Adv. Funct. Mater*, 2015, **25**, 597.

8 C. Ruan, K. Ai, X. Li, L. Lu, *Angew. Chem. Int. Ed*, 2014, **53**, 5556.

9 C. Wu, X. Huang, X. Wu, R. Qian, P. Jiang, *Adv. Mater*, 2013, **25**, 5658.

10 L. Feng, Z. Zhang, Z. Mai, Y. Ma, B. Liu, L. Jiang, D. Zhu, *Angew. Chem. Int. Ed*, 2004, **43**, 2012.

11 C. H. Lee, N. Johnson, J. Drelich, Y. K. Yap, *Carbon*, 2011, **49**, 669.

12 X. Zhang, Z. Li, K. Liu, L. Jiang, *Adv. Funct. Mater*, 2013, **23**, 2881.

13 H. Bi, Z. Yin, X. Cao, X. Xie, C. Tan, X. Huang, B. Chen, F. Chen, Q. Yang, X. Bu, X. Lu, L. Sun, H. Zhang, *Adv. Mater*, 2013, **41**, 5916.

14 X. Gui, J. Wei, K. Wang, A. Cao, H. Zhu, Y. Jia, Q. Shu, D. Wu, *Adv. Mater*, 2010, **22**, 617.

15 M. W. Lee, S. An, S. S. Latthe, C. Lee, S. Hong, S. S. Yoon, *ACS Appl. Mater. Interfaces*, 2013, **5**, 10597.

16 Y. Hu, X. Liu, J. Zou, T. Gu, W. Chai, H. Li, *ACS Appl. Mater. Interfaces*, 2013, **5**, 7737.

17 D. Deng, D. P. Prendergast, J. MacFarlane, R. Bagatin, F. Stellacci, P. M. Gschwend, *ACS Appl. Mater. Interfaces*, 2013, **5**, 774.

18 P. Calcagnile, D. Fragouli, I. S. Bayer, G. C. Anyfantis, L. Martiradonna, P. D. Cozzoli, R. Cingolani, A. Athanassiou, *ACS Nano*, 2012, **6**, 5413.

19 B. Wang, J. Li, G. Wang, W. Liang, Y. Zhang, L. Shi, Z. Guo, W. Liu, *ACS Appl. Mater. Interfaces*, 2013, **5**, 1827.

20 Y. Cao, X. Zhang, L. Tao, K. Li, Z. Xue, L. Feng, Y. Wei, *ACS Appl. Mater. Interfaces*, 2013, **5**, 4438.

21 J. Yuan, X. Liu, O. Akbulut, J. Hu, S. L. Suib, J. Kong, F. Stellacci, *Nat. Nanotechnol*, 2008, **3**, 332.

22 G. Ju, M. Cheng, M. Xiao, J. Xu, K. Pan, X. Wang, Y. Zhang, F. Shi, *Adv. Mater*, 2013, **25**, 2915.

23 J. Zhang, S. Seeger, *Adv. Funct. Mater*, 2011, **21**, 4699.

24 D. Zang, C. Wu, R. Zhu, W. Zhang, X. Yu, Y. Zhang, *Chem. Commun*, 2013, **49**, 8410.

25 X. Zhou, Z. Zhang, X. Xu, F. Guo, X. Zhu, X. Men, B. Ge, *ACS Appl. Mater. Interfaces*, 2013, **5**, 7208.

26 H. Bi, X. Xie, K. Yin, Y. Zhou, S. Wan, L. He, F. Xu, F. Banhart, L. Sun, R. S. Ruoff, *Adv. Funct. Mater*, 2012, **22**, 4421.

27 A. K. Sasmal, C. Mondal, A. K. Sinha, S. S. Gauri, J. Pal, T. Aditya, M. Ganguly, S. Dey, T. Pal, *ACS Appl. Mater. Interfaces*, 2014, **6**, 22034.

28 A. Asthana, T. Maitra, R. Büchel, M. K. Tiwari, D. Poulikakos, *ACS Appl. Mater. Interfaces*, 2014, **6**, 8859.

29 S. Huang, *ACS Appl. Mater. Interfaces*, 2014, **6**, 17144.

30 Q. Ke, Y. Jin, P. Jiang, J. Yu, *Langmuir*, 2014, **30**, 13137.

31 Q. Zhu, Q. Pan, *ACS Nano*, 2014, **8**, 1402.

32 Y. Yang, H. Li, S. Cheng, G. Zou, C. Wang, Q. Lin, *Chem. Commun*, 2014, **50**, 2900.

33 J. Y. Huang, S. H. Li, M. Z. Ge, L. N. Wang, T. L. Xing, G. Q. Chen, X. F. Liu, S. S. Al-Deyab, K. Q. Zhang, T. Chen, Y. K. Lai, *J. Mater. Chem. A*, 2015, **3**, 2825.

34 J. Li, L. Shi, Y. Chen, Y. Zhang, Z. Guo, B. Su, W. Liu, *J. Mater. Chem*, 2012, **22**, 9774.

35 F. Wang, S. Lei, M. Xue, J. Ou, C. Li, W. Li, *J. Phys. Chem. C*, 2014, **118**, 6344.

36 B. Li, L. Wu, L. Li, S. Seeger, J. Zhang, A. Wang, *ACS Appl. Mater. Interfaces*, 2014, **6**, 11581.

37 C. Wang, F. Tzeng, H. Chen, C. Chang, *Langmuir*, 2012, **28**, 10015.

38 L. Kong, X. Chen, L. Yu, Z. Wu, P. Zhang, *ACS Appl. Mater. Interfaces*, 2015, **7**, 2616.

39 J. Gu, P. Xiao, Y. Huang, J. Zhang, T. Chen, *J. Mater. Chem. A*, 2015, **3**, 4124.

40 Z. Xue, S. Wang, L. Lin, L. Chen, M. Liu, L. Feng, L. Jiang, *Adv. Mater*, 2011, **23**, 4270.

41 X. Gao, L. Xu, Z. Xue, L. Feng, J. Peng, Y. Wen, S. Wang, X. Zhang, *Adv. Mater*, 2014, **26**, 1771.

42 L. Zhang, Z. Zhang, P. Wang, *NPG Asia Mater*, 2012, **4**, e8.

43 Y. Sawai, S. Nishimoto, Y. Kameshima, E. Fujii, M. Miyake, *Langmuir*, 2013, **29**, 6784.

44 F. Zhang, W. B. Zhang, Z. Shi, D. Wang, J. Jin, L. Jiang, *Adv. Mater*, 2013, **25**, 4192.

45 S. Zhang, F. Lu, L. Tao, N. Liu, C. Gao, L. Feng, Y. Wei, *ACS Appl. Mater. Interfaces*, 2013, **5**, 11971.

46 W. Zhang, Y. Zhu, X. Liu, D. Wang, J. Li, L. Jiang, J. Jin, *Angew. Chem. Int. Ed*, 2014, **53**, 856.

47 Y. Cao, N. Liu, C. Fu, K. Li, L. Tao, L. Feng, Y. Wei, *ACS Appl. Mater. Interfaces*, 2014, **6**, 2026.

48 Q. Liu, A. A. Patel, L. Liu, *ACS Appl. Mater. Interfaces*, 2014, **6**, 8996.

49 X. Zheng, Z. Guo, D. Tian, X. Zhang, W. Li, L. Jiang, *ACS Appl. Mater. Interfaces*, 2015, **7**, 4336.

50 Y. Li, W. Jia, Y. Song, X. Xia, *Chem. Mater*, 2007, **19**, 5758.

51 A. Lafuma, D. Quéré, *Nat. Mater*, 2003, **2**, 457.

52 P. Roach, N. J. Shirtcliffe, M. I. Newton, *Soft Matter*, 2008, **4**, 224.

53 X. Zhang, F. Shi, J. Niu, Y. Jiang, Z. Wang, *J. Mater. Chem*, 2008, **18**, 621.

54 V. A. Ganesh, H. K. Raut, A. S. Nair, S. Ramakrishna, *J. Mater. Chem*, 2011, **21**, 16304.

55 X. Deng, L. Mammen, H. Butt, D. Vollmer, *Science*, 2012, **335**, 67.

56 R. N. Wenzel, *Ind. Eng. Chem*, 1936, **28**, 988.

57 M. Liu, S. Wang, Z. Wei, Y. Song, L. Jiang, *Adv. Mater*, 2009, **21**, 665.

58 J. P. Youngblood, T. J. McCarthy, *Macromolecules*, 1999, **32**, 6800.